Kovove Mater. 49 2011 207–212
DOI: 10.4149/km_2011_3_207

The skin effect in a high pressure die cast Mg-La alloy

K. V. Yang[1]*, C. H. Cáceres[1], M. A. Easton[2], M. A. Gibson[3]

[1] *ARC Centre of Excellence for Design in Light Metals, Materials Engineering, School of Engineering, The University of Queensland, QLD-4072, Australia*
[2] *CAST Co-operative Research Centre, Department of Materials Engineering, Monash University, Melbourne, VIC-3800, Australia*
[3] *CAST Co-operative Research Centre, CSIRO Process Science and Engineering, Clayton, VIC-3169, Australia*

Received 8 December 2010, received in revised form 1 April 2011, accepted 6 April 2011

Abstract

Cross-sectional microhardness maps of high pressure die cast-to-shape specimens of a Mg--3.44mass%La alloy with either rectangular or circular cross-section were produced. A harder layer, or "skin", was observed near the casting surface in both cross-sectional shapes. The higher hardness values were ascribed to the finer solidification microstructure and higher volume fraction of eutectic in the skin. The lower hardness values observed at the centre, or "core", of the cross-section were ascribed to the larger average grain size resulting from the aggregation of externally solidified grains and dispersed microporosity. The skin was non--uniform in both depth and hardness due to local homogeneities of the grain microstructure caused by the scattered presence of large externally solidified grains near the surface, for both geometries, but especially for the rectangular one. The global and local features of the skin appear related to the distribution of the externally solidified grains as determined by the solidification pattern characteristic to geometry of the die cross-section.

K e y w o r d s: magnesium-RE alloys, grain microstructure, high pressure die casting, skin effect, microhardness mapping

1. Introduction

Mg-RE alloys are receiving increased attention due to their higher creep resistance [1], and the study of the binary alloys involving the individual RE components is an important step forward in understanding the microstructure-properties relationship in these alloys [2]. The eutectic morphology and average volume fraction of intermetallics in three binary Mg-RE (Ce, La and Nd) alloys were recently reported by Chia et al. [2], but a detailed characterisation of these alloys' microstructure is still lacking.

A harder surface layer, or casting "skin", is normally observed in cold chamber high pressure die cast (HPDC) Mg alloys [3–6]. In Mg-Al alloys [7, 8] the skin exhibits higher integrity and hardness. The latter is ascribed to the combination of very fine α-Mg grains, greater volume fraction of the β ($Mg_{17}Al_{12}$) – intermetallic phase and increased supersaturation of Al in the α-Mg. The solid solubility of the RE elements in Mg is much lower than that of Al, and the solidification behaviours of Mg-Al and Mg-RE alloys differ widely despite the basic similarity of the phase diagrams. Lanthanum represents an extreme case within the RE family due to its very low solubility, and for this reason a Mg-La alloy was chosen for the present study. Like the Mg-Al, the Mg-La system forms an eutectic at the Mg-rich end, with some major differences [9]: the maximum solubility of La in Mg is only ~ 0.23 mass% compared with Al of ~ 11.5 mass%; the eutectic temperature in the Mg-La system is much higher, at $\sim 612\,^{\circ}C$ compared to $\sim 437\,^{\circ}C$ for Mg-Al; the eutectic composition is lower at approximately 16.5 mass% in the Mg-La system against 31 mass% in the Mg-Al system; the eutectic morphology is lamellar with alternating layers of α-Mg and $Mg_{12}La$ [2] in Mg-La whereas the eutectic in Mg-Al is divorced or partially divorced [10]. The skin and core regions of the casting cross section of Mg-La alloys can be thus expected to reflect

*Corresponding author: tel.: + 61 (0) 7 3346 9571; fax: + 61 (0) 7 3365 3888; e-mail address: kun.yang@uq.edu.au

these differences in comparison with the Mg-Al alloys.

In this work microhardness mapping of the entire cross-sections of specimens of an HPDC Mg-La alloy with two different cross-sectional shapes was used to determine the characteristics of the skin and to assess the effect of the die shape on the overall grain and eutectic microstructure.

2. Materials and experimental details

The specimens used in this study were from the same set used in the study by Chia et al. [2]. The binary Mg-3.44mass%La alloy was produced from commercial purity magnesium and lanthanum. The melt was held at 740 ℃ until transferred to the shot sleeve. The melt was protected using AM-Cover (0.2 % tetrafluoroethane in 99.8 % nitrogen). The alloys were cast into a three-cavity die through a trapezoidal runner of 12 mm in height with the parallel faces being 11 mm and 14 mm, which tapers towards the castings using a 250 T Toshiba cold chamber HPDC machine. A rectangular dog-bone shaped tensile specimen (5.75 mm width and 3 mm thickness) and two with a circular (5.65 mm diameter) cross-section were made on each shot. The specimens' gates were approximately 15 mm^2 in area. The maximum ram velocity was 2.25 $m\,s^{-1}$ and the intensification pressure was 120 MPa. The die cavity was filled in approximately 600 ms.

Samples for microhardness testing and microstructural characterization were sectioned from the centre of undeformed specimens and polished down to 0.05 μm colloidal silica. Microhardness was measured using an automated Vickers tester, with a load of 50 gram-force and a dwell time of 12 s. The microhardness mapping covered the entire cross-section of the samples, as illustrated by the indentation patterns in Figs. 1a,b. A minimum distance of 100 μm was set between adjacent indentations or away from the free surface, in agreement with the ASTM E384-07 norm, by which adjacent indentations must be at least 2.5 times the indentation diagonal (predetermined to be around 40 μm) apart. After testing, a 3D hardness surface map was created using a commercial software package (Surfer). The microstructures were studied using a JEOL 6460 SEM, on sections adjacent to those used for the microhardness testing.

3. Results

3.1. Microhardness behaviour

The microhardness maps of Figs. 1c,d show that higher hardness values, within the range 75–100 HV, generally followed the periphery of the cross-sections, roughly identifying the skin for both geometries. The skin appeared generally patchy and non-uniform in both strength and depth, for either geometry, but especially in the rectangular, in which the hardness was highest at the corners, lower at the centre of the long edges and lowest at the core. The average hardness of the skin on opposite sides of the cross-sections was different, indicating that the skin was asymmetric, for both geometries. The most obvious difference between the two shapes was that the cylindrical specimen's skin was much more uniform and continuous.

A very few points with low hardness number, in the range 30–45 HV, were found in the core region for both shapes. These low values are normally ascribed to shrinkage and gas micro porosity [8], and, as can be seen in Figs. 1a,b (see also Figs. 3a,b), that was also the case in the present work.

For the rectangular cross-section, the indentation points were sorted into two groups; the E (edge) regions and the C (centre) region, as described in Fig. 2a. Within each region, the average microhardness values for given y were plotted in Fig. 2b as a function of their y-coordinate (termed distance from the top surface in Fig. 2a). The maximum difference in hardness between the centre and the edge was about 33 HV.

For the cylindrical specimen, the average hardness values for given radial distance were plotted in Fig. 2c. The hardness showed a similar trend as for the rectangular specimen and with a similar maximum span of values of ~ 33 HV. In Fig. 2d, the average hardness has been plotted on a common x-axis scale to show that although the spatial behaviours were generally similar, the skin was much better defined in the cylindrical specimen. The weighted average hardness values for the entire cross-sections were 67.2 HV (rectangular) and 71.5 HV (cylindrical).

3.2. Microstructure

Figures 3a,b show macrographs of the entire cross--sections, Fig. 3c compares the microstructure at the corner, surface and core regions for the rectangular specimen, and Fig. 3d does the same for the surface and core for the cylindrical specimen. The images in the latter case were collected in sets for given radial distance. In both specimens the microstructure consisted of primary α-Mg solid solution, which appeared dark, in the form of either small equiaxed grains or large dendritic grains, and intergranular eutectic colonies, which appeared bright.

Two macrosegregation bands, showing in Figs. 3a,b as bright rings, were observed in both specimens, with features pertinent to each geometry: in the cylindrical specimen, one band can be seen very close to the casting surface and a second, more diffuse one, appeared

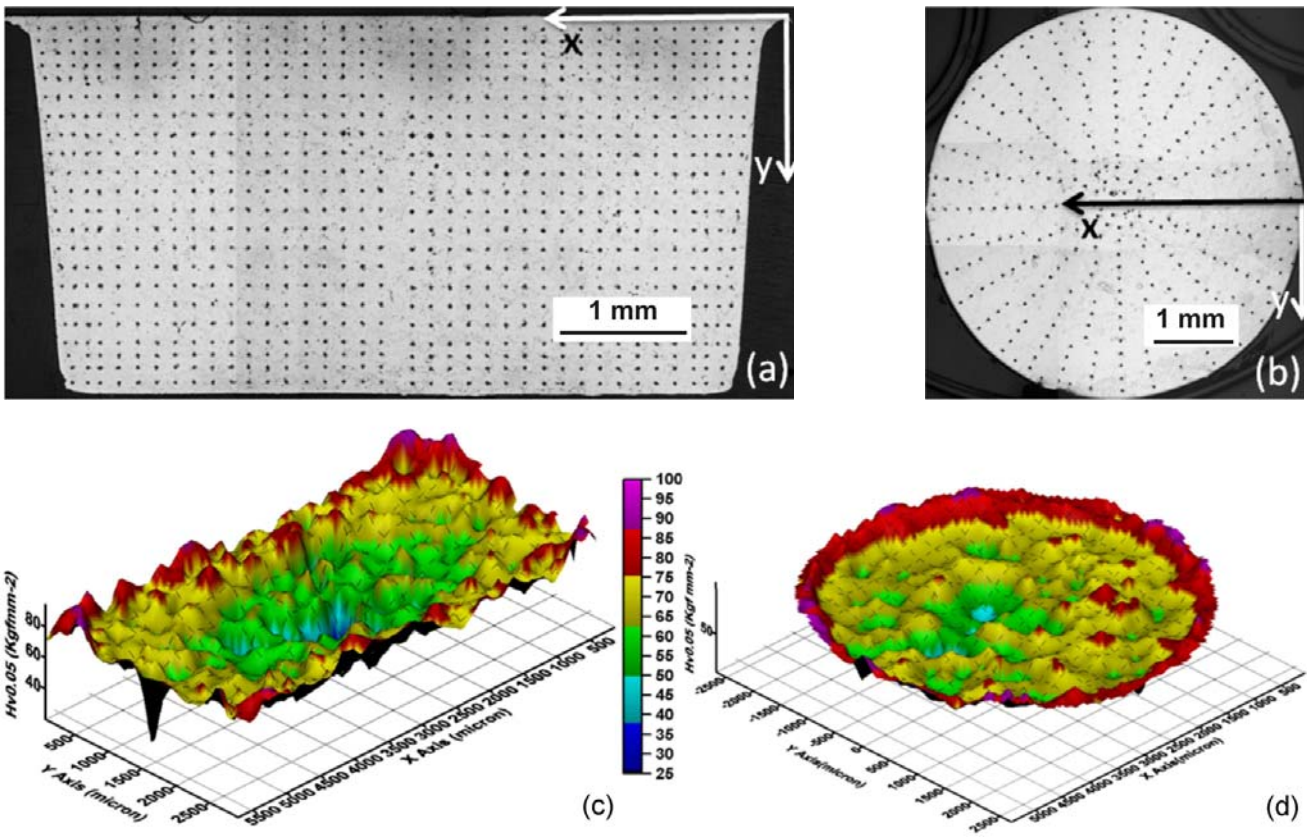

Fig. 1. Indentation patterns for (a) the rectangular specimen and (b) the cylindrical specimen and (c), (d) microhardness maps with a common colour scale for both cross-sections.

near the centre; in the rectangular one, the outermost band was fragmented and visible only near the corners of the section, whereas the inner one was visible as an elliptical ring. Some scattered microporosity was observed as well, especially at the core. Large dendritic grains were prevalent at the core of both sections, Figs. 3c,d, whereas small primary α-Mg grains prevailed at the surface of the circular section and at the corners of the rectangular one. A few large grains were also observed scattered near the surface, especially in the rectangular specimen.

4. Discussion

The good thermal contact between the die wall and the solidifying metal ensured by the applied pressure during solidification and the relatively low heat capacity of the molten magnesium results in cooling rates as high as 400–500 $\mathrm{K\,s^{-1}}$ [11, 12], creating a very fine microstructure near the casting surface. This is normally considered to be the reason for the formation of the harder "skin". This interpretation suggests that the skin should follow the casting contour closely reproducing the shape of the die. By extension, the skin is implicitly assumed to be continuous. The microhardness maps of Fig. 1 show that to a large extent, and unlike for the rectangular specimen, a continuous skin does form in the cylindrical specimen. It is noted in passing that these features broadly agree with the description of the skin in similar shape specimen of AZ91 alloy [8].

It is known that the large dendritic grains observed in Figs. 3c,d, often called externally solidified α-Mg grains (ESG's) [13], are due to the premature solidification in the shot sleeve and runner. Their presence in the die cavity results in a bimodal distribution of α-Mg grain sizes [14] with a prevalence of ESG's at the core region. The lower hardness values at the core can thus be partly ascribed to the locally larger grain size, for both die geometries.

On a closer look, Figs. 3c,d show that ESG's also appeared stochastically distributed at the skin regions. This locally non-uniform grain microstructure near the surface was reflected by the local unevenness of the skin in the maps of Figs. 1c,d. In the case of the rectangular specimen, no ESG's were found at the corners (Figs. 3a,c), hence the higher hardness, whereas they were seen in larger concentrations at the middle of the edges, thus accounting for the somewhat lower and uneven hardness. Figure 3d shows that in the cylindrical specimen there were very few ESG's near the surface, accounting for the more continuous and uniform skin in Fig. 1d. Thus, in principle, the

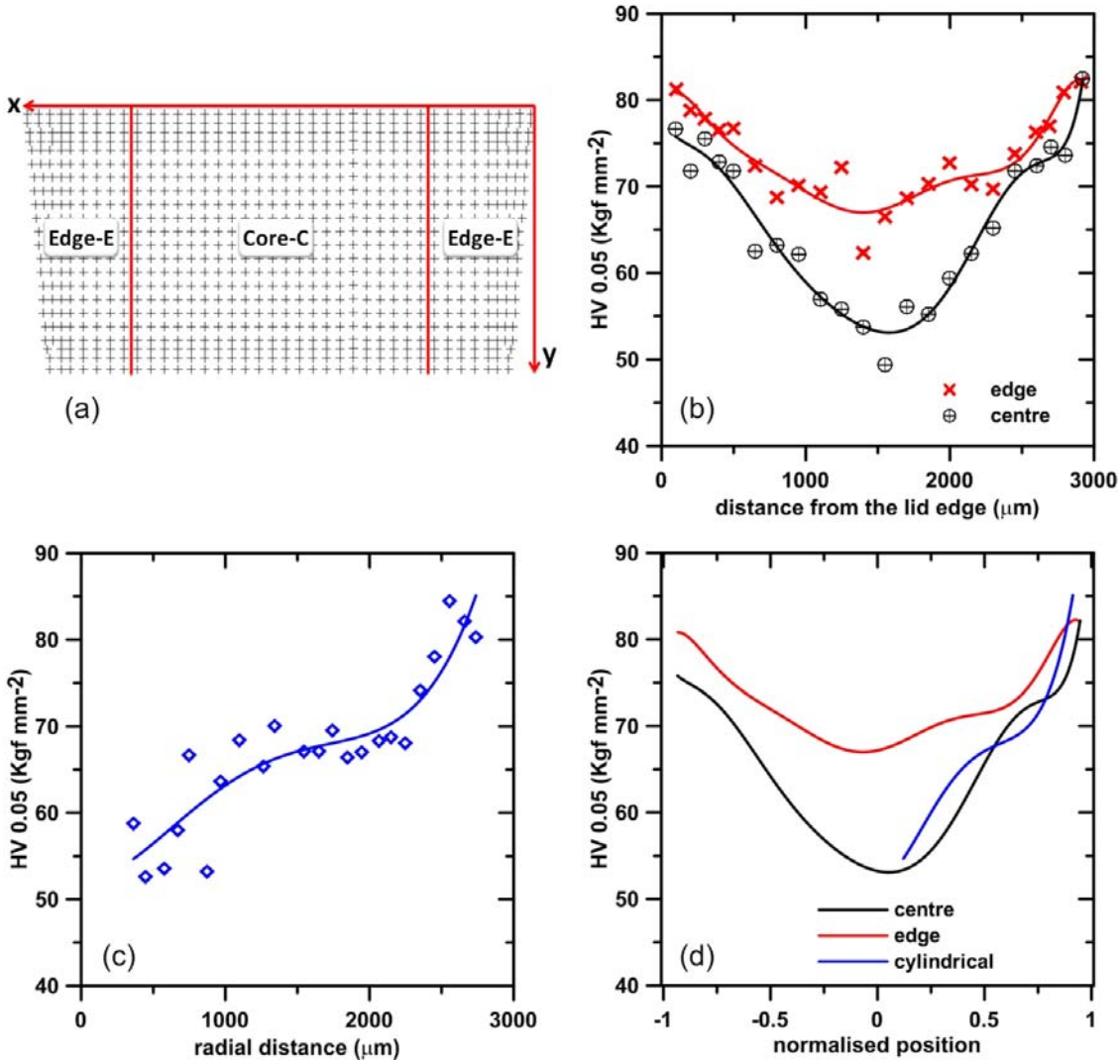

Fig. 2. (a) Diagram identifying the edge and centre regions of the rectangular specimen; (b), (c) the hardness averaged over all points at a given distance from the top surface of the rectangular specimen or the radial distance for the cylindrical one, respectively; (d) lines of best fit to the data of Figs. 2b,c as a function of the normalised distance from the centre of the sections.

distribution of ESG's accounts for the global and local features of the skin hardness profile in either geometry.

The distribution of the ESG's can be easily related to the rheology of the die filling and the solidification pattern characteristic to each cross sectional geometry. According to Laukli et al. [13] the ESG's tend to migrate to the centre of the casting driven by the constraint created by the thin surface layer that solidifies first against the die wall. In the cylindrical specimen the heat extraction is radial and solidification can be expected to progress uniformly towards the centre once the filling is complete. The ESG's can thus be expected to agglomerate at the core, as indeed observed in Figs. 3b and 3d. In the rectangular cross-section, a higher cooling rate can be expected at the corners because of the locally higher specific surface area. A solidification front can thus be expected to form first there once the die fills, pushing the ESG's towards the central section. The distribution of ESG's in Fig. 3c identifies the ESG's final migration stage during solidification, and it is seen that although they tend to concentrate at the core, they also spread towards the long edges of the section. The lack of uniformity of the skin along the flat surfaces and the higher hardness values at the corners in the map of Fig. 1c follow.

5. Summary

Microhardness mapping was used to characterize the skin in an HPDC Mg-3.44mass%La alloy, cast with rectangular and cylindrical cross sections. The hardness was generally higher near the casting surface, or skin, than at the centre, or core, of the cross-section

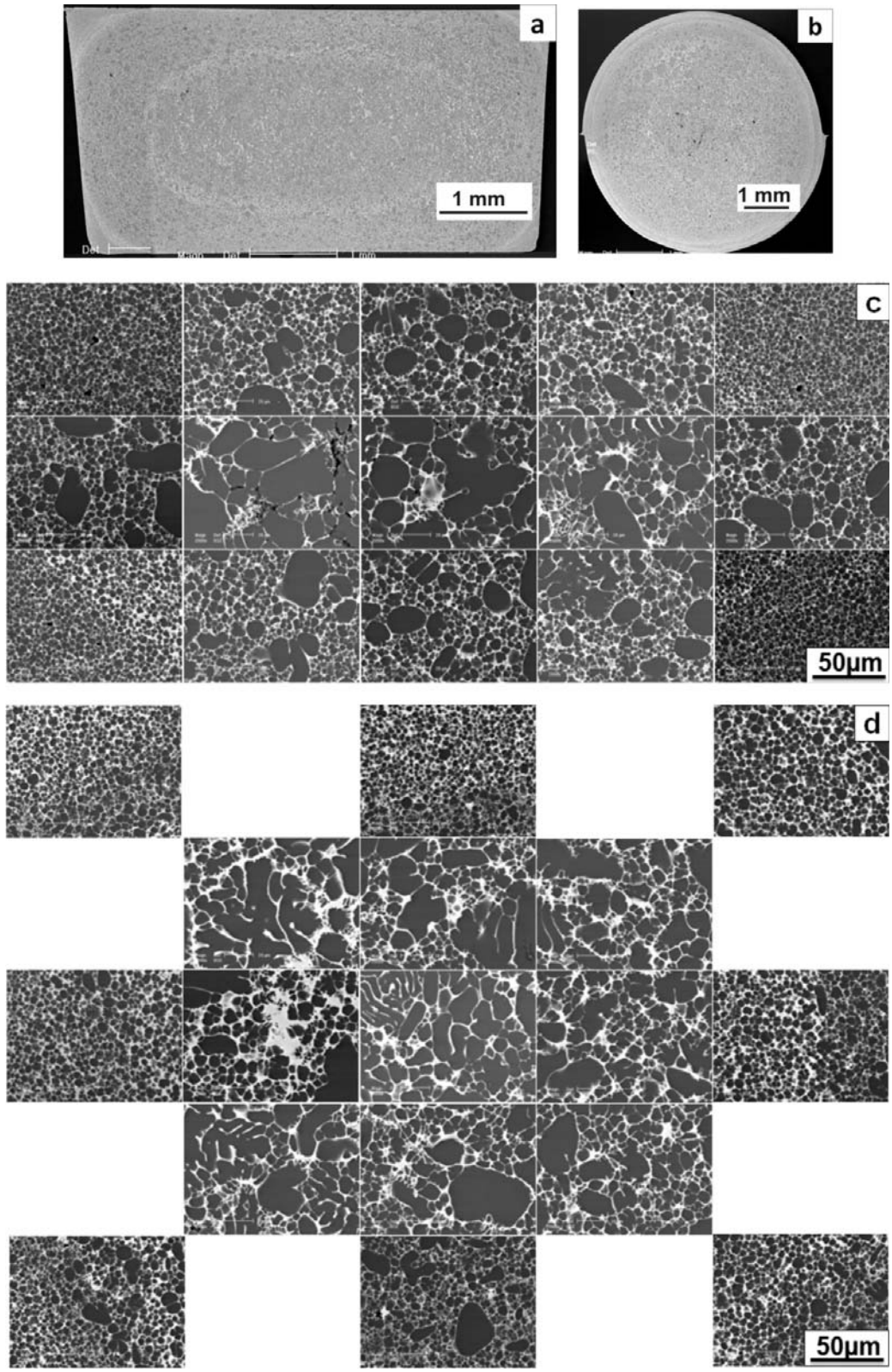

Fig. 3. (a), (b) Back scattered electron images of the full cross-sections; (c), (d) higher magnification images at selected locations, of the rectangular and circular cross-sections, respectively. See text for details.

irrespective of the shape. This behaviour was accounted for by the finer grain microstructure at the skin and the coarser solidification microstructure and the concentration of porosity at the core.

The geometry of the cross-section relative to the casting rheology and the solidification pattern appeared to determine both the local and global features of the skin through the distribution of ESG's. In the cylindrical specimen the die filling and solidification pattern naturally matched the shape of the cross-section. The large dendritic grains were segregated to the core whereas uniformly fine grains formed near the casting surface; hence relatively continuous and uniform the skin. In the rectangular specimen the solidification started at the corners, and a positive gradient in the concentration of ESG's resulted in a more discontinuous and non-uniform skin, both in hardness and depth.

References

[1] ZHU, S. M.—GIBSON, M. A.—EASTON, M. A.—NIE, J. F.: Scripta Materialia, *63*, 2010, pp. 698–703. doi:10.1016/j.scriptamat.2010.02.005

[2] CHIA, T. L.—EASTON, M. A.—ZHU, S. M.—GIBSON, M. A.—BIRBILIS, N.—NIE, J. F.: Intermetallics, *17*, 2009, p. 481. doi:10.1016/j.intermet.2008.12.009

[3] SEQUEIRA, W. P.—MURRAY, M. T.—DUNLOP, G. L.—StJOHN, D. H.: TMS Symposium on automotive alloys, 1997, p. 169.

[4] WEILER, J. P.—WOOD, J. T.—CLASSEN, R. J.—BERKMORTEL, R.—WANG, G.: Materials Science and Engineering A, *419*, 2006, p. 297. doi:10.1016/j.msea.2006.01.034

[5] SONG, J.—XIONG, S.-M.—LI, M.—ALLISON, J.: Materials Science and Engineering A, *520*, 2009, p. 197. doi:10.1016/j.msea.2009.05.042

[6] PETTERSEN, G.—HOIER, R.—LOHNE, O.—WESTENGEN, H.: Materials Science and Engineering, *207A*, 1996, p. 115.

[7] YANG, K.—NAGASEKHAR, A. V.—CACERES, C. H.: Advanced Materials Research, *97–101*, 2010, p. 743.

[8] CACERES, C. H.—GRIFFITHS, J. R.—PAKDEL, A. R.—DAVIDSON, C. J.: Materials Science and Engineering, *402*, 2005, p. 258. doi:10.1016/j.msea.2005.04.042

[9] ROKHLIN, L. L.: Magnesium Alloys Containing Rare Earth Metals. New York, Taylor & Francis 2003.

[10] DAHLE, A. K.—LEE, Y. C.—NAVE, M. D.—SCHAFFER, P. L.—StJOHN, D. H.: Journal of Light Metals, *1*, 2001, p. 61. doi:10.1016/S1471-5317(00)00007-9

[11] SEQUEIRA, W. P.—DUNLOP, G. L.—MURRAY, M. T.: In: 3rd International Magnesium Conference, London. Ed.: Lorimer, G. W. London, The Institute of Metals 1997, p. 63.

[12] DARGUSCH, M. S.—NAVE, M.—McDONALD, S. D.—StJOHN, D. H.: Journal of Alloys and Compounds, *492*, 2010, p. L64. doi:10.1016/j.jallcom.2009.11.199

[13] LAUKLI, H. I.—GOURLAY, C. M.—DAHLE, A. K.: Metallurgical and Materials Transactions A: Physical Metallurgy and Material Science, *36*, 2006, p. 805. doi:10.1007/s11661-005-1011-5

[14] NAGASEKHAR, A. V.—EASTON, M. A.—CACERES, C. H.: Advanced Engineering Materials, *11*, 2009, p. 912. doi:10.1002/adem.200900175